Journal of Engineering Research and Education
Volume 17, 2025 [125-139]

New Design Mechanism Four-Bit Control of Variable Twist Angle Single Module for Adding Industrial Robot Wrist Dexterity

Amir Sharizam Ismail[1,] , Samsi Md Said[2] , Tengku Mohd Azahar Tuan Dir[3] and Jamel Othman[4]

[1,2,3,4]Mechatronics Engineering Technology Section, Universiti Kuala Lumpur Malaysia France Institute, Bandar Baru Bangi, Selangor, Malaysia

ABSTRACT

This study focuses on hyper-redundant robots, which are highly articulated and connected to industrial robots. These robots have a higher degree of freedom, allowing for infinite configuration and delivering points of interest. However, they require complex universal joints and linkages systems, which can be challenging to design. To address this, a variable twist angle module with a high-compliant flexible joint is proposed. The concept of binary control for two-dimensional truss systems is modified to work with industrial robots, and a new mathematical compression of four degrees of freedom robotic system into a single module arm matrix is implemented. The virtual Robot Experimental Platform is used for physical and controller modeling. The study concludes that hyper-redundant robots provide solutions with dexterity, even with fault tolerance as the task-space dimension.

Keywords: Parallel Joint, Industry Robot, Degree of Freedom, Kinematic Model

1. INTRODUCTION

Industrial robots are commonly linked to technological progress in the 21st century. Nevertheless, their beginnings may be traced back to an earlier period, specifically the 1950s, when George Devol [1] pioneered the first industrial robot. This groundbreaking invention was a colossal two-ton apparatus that employed hydraulic actuators to independently move products from one place to another. As sensors, electronics, and computer software have improved, industrial robots have greatly increased their capacities, allowing them to do intricate jobs like assembly and inspection. In the future, as industrial robots advance in intelligence, they will possess the capability to do more complex jobs with superior efficiency compared to humans. Furthermore, they will possess the capability to function securely in conjunction with people inside manufacturing environments. An exemplary instance of contemporary industrial robotics is the hyper-redundant robots or manipulators [2], [3].

Hyper-redundant robots are robotic systems that include a significant or unlimited number of redundant components in terms of their movement and/or actuators. The degree of freedom is a critical factor in hyper-redundant robots, since it determines the number of separate motions, they can perform. Hyper-redundant robots have a higher number of degrees of freedom compared to ordinary robots. These robots demonstrate extraordinary mastery of their body movement and configurations, enabling the end effector to consistently retain its position, location, and orientation. Hyper-redundant robots possess exceptional body control and orientation, enabling them to do a diverse array of activities. These jobs include conducting inspections in cramped locations, employing inventive grasping and locomotion techniques, executing precise manipulation and handling of items, and accessing restricted regions.

*amirsharizam@unikl.edu.my

The significance of a new design mechanism using 4-bit control for a variable twist angle single module in industrial applications depends on several factors. Here's a breakdown of the potential benefits and considerations:

i. Simplified Control for Complex Movements: The 4-bit control system effectively utilizes the four actuators to achieve a wider range of motion or specific movement patterns compared to traditional methods, it could be beneficial for tasks required.
ii. Reduced Control Complexity: The 4-bit control significantly simplifies the control algorithms compared to traditional methods for achieving similar movements with four actuators.
iii. Considerations for Industrial Applications.

2. HYPER REDUNDANT ROBOT MANIPULATOR

Zhao designs an open-structured hyper-redundant elephant's trunk robot (HRETR) [4], [5], as seen in Figure 1. Mechanical structure design, kinematic analysis, control system design, virtual prototype simulation, and prototype construction are the main areas of study for them. The design of the elephant's trunk, composed of six-unit modules known as 3UPS-PS parallel in series, was inspired by its flexible and expansive action. The mechanical design of the HRETR is derived on the concept of mechanical bionic design and draws inspiration from the locomotion traits of an elephant's trunk. Subsequently, the backbone mode technique is employed to construct the kinematic model of the robot. The simulation tools SolidWorks and ADAMS [6], [7] are combined to evaluate the kinematic characteristics while assigning the trajectory of the robot's end-moving platform. The ANSYS software is utilised to evaluate the static stiffness of individual components as well as the whole robot. The selection of materials for the weak sections of the mechanical structure and the hardware is done meticulously based on this principle. Then, modular and hierarchical design principles are used to build the extensible structures of hardware and software control systems. In the end, the prototype is constructed, and its functionality is evaluated. A strategy to creating and building a hyper-redundant bionic system is described in the proposed research.

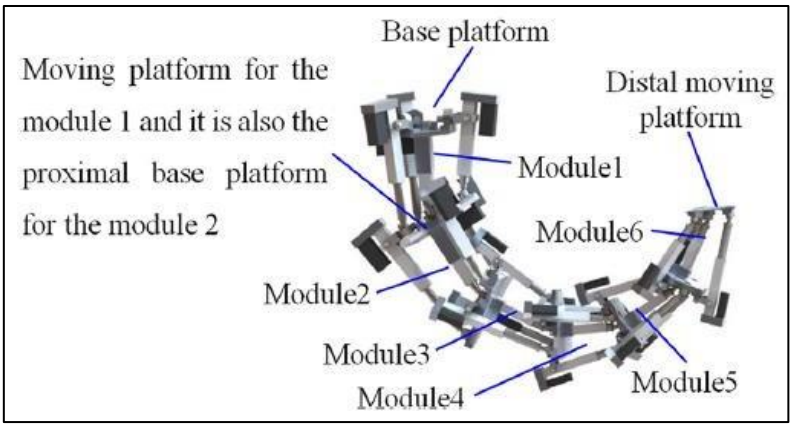

Figure 1. Hyper-Redundant Elephant's Trunk Robot

Martín-Barrio presents a unique blueprint for a highly redundant manipulator with fourteen degrees of freedom and seven components manipulated shows in Figure 2 by cables [8]–[10]. The system prioritizes reliability, precision, and delicacy in moving payloads. Effective regulation ensures efficient control from actuators to form management. However, intricate forms can hinder their perception in space. Immersive technology is a feasible choice for remote and secure control in dangerous areas. Experimental findings confirm the validity of the proposed robot

design and control approaches, indicating that hyper-redundant robots and immersive technologies will play a significant role in future automated and remote applications.

Figure 2. Tendon-Driver, Discrete and Hyper-Redundant Manipulator

Tang et al have developed a cable-driven hyper-redundant robot using a multi-segmented construction, allowing for two degrees of freedom. The robot is divided into segments with three spherical-prismatic-spherical chains and a universal joint chain (3-SPS-U). Kinematics analysis is performed between the actuator and joint space, resulting in a model of a parallel mechanism with four chains. Geometric principles are used to establish coordinate frames, allowing for direct acquisition of forward kinematics from joint space to task space. The product of exponentials method is employed for inverse kinematics analysis. A prototype with 24 degrees of freedom, consisting of 12 components and 36 cables, is produced shows in Figure 3 and an experimental platform for real-time robot control is created [11], [12].

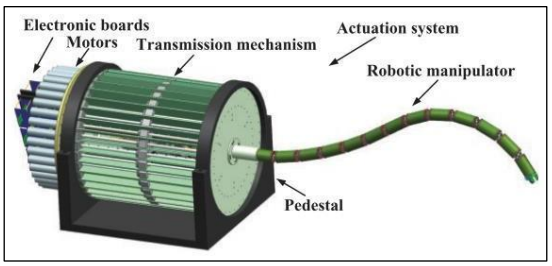

Figure 3. Tendon-Driver, Discrete and Hyper-Redundant Manipulator

Ciprian Lapusan is studying the forward kinematic analysis of a hyper-redundant robot designed for vertical agricultural inspections and harvesting tasks. The robot, consisting of seven Three-Revolute Prismatic Spherical parallel modules with 21 degrees of freedoms shows in Figure 4, is highly suitable for these tasks due to its agility and ability to adjust to various unstructured scenarios. The study focuses on the forward kinematics of a single module, followed by a comprehensive investigation of the entire structure and MATLAB code evaluation using a simulated robot model [13], [14].

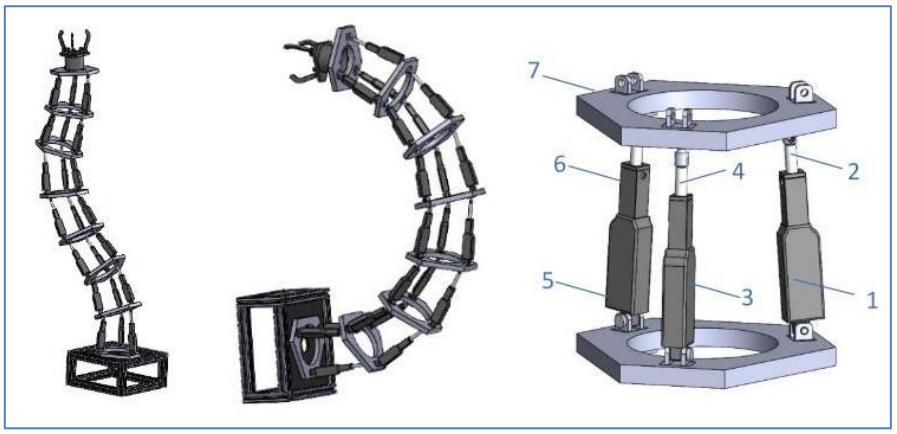

Figure 4. CAD 3-RPS (Revolute-Prismatic-Spherical) Parallel Modules

2.1 Parallel Module

Lafmejani has developed a multi-segment model that replicates all fundamental movements of an octopus arm, including elongation, contraction, bending, and twisting shows in Figure 5. The model is evaluated by simulating various 3D reference trajectories, including straight lines, ellipses, sinusoidal paths, and octopus-like reaching and fetching movements, to ensure its effectiveness [15], [16].

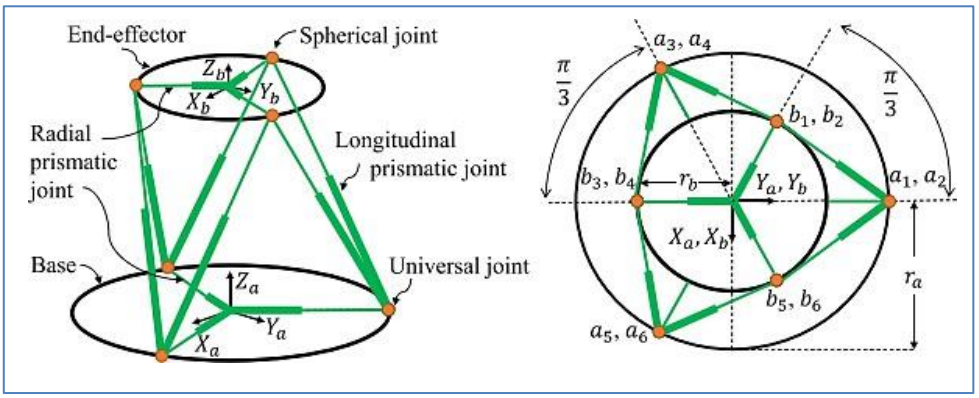

Figure 5. Parallel Modules Hyper-Redundant Robot Single Segment Model Based on a UPS 6-DOF Gough-Stewart (GS) Platform

Hyper-redundant manipulators provide exceptional flexibility and maneuverability, enabling them to operate well in restricted spaces. They have a diverse variety of applications in complex situations. Their study encompassed the definition, classification, kinematics approach, method for calculating workspace, trajectory planning, and algorithm for planning obstacle avoidance routes for Hyper-redundant manipulators.

The objective is to establish a connection between academic researchers and the present condition of Hyper-redundant manipulators. Additionally, the aim is to compile the primary algorithms used in solving kinematics, calculating workspace, planning trajectories, and avoiding obstacles in the path of ultra-redundant robots that have been developed in the past ten years. The technological challenges and potential advancements of the Hyper-redundant manipulator are discussed in detail.

3. KINEMATIC MODEL OF SINGLE MODULE

The Denavit – Harternberg model and parameters are used to define the geometry of rigid body attachments to their parent. This attempt involves creating robot segments or modules, which will be linked together to form an assembly for a multi-degrees-of-freedom hyper-redundant robot. A single module is usually treated as a degree of freedom using four arm matrices [17].

The module is made up of an orientation disc and a reference disc. The NOAP orientation axis is on the outside disc, and the XYZ axis is attached to the reference disc. The X-axis origins are equal to arm's length, denoted as 'a'. The offset distance is 0 since there is no movement along the Z axis. The twist angle α is determined by prismatic actuators, with different values resulting in a comparable angular variable θ.

The four-bar linkage mechanism utilizes the bang-bang control technique to demonstrate the impact of twist angle change on the NOAP homogenous orientation and position matrix, as seen in Figure 6.

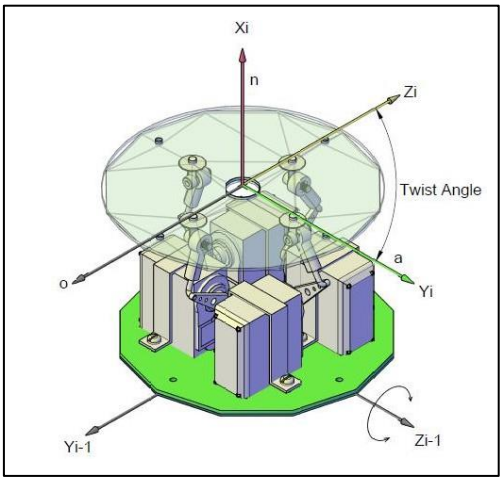

Figure 6. Variable Twist Angle Module

The Denavit-Hartenberg modelling approach consists of four consecutive transformations of axes, labelled from (1) to (4).

$[Z_i] = Translation[z_{i-1}, d_i]\ Rotation\ [z_{i-1}, \theta_i]\ is\ the\ z_{i-1}\ rotary\ motion\ and;$
$[X_i] = Translation\ [n_i, a_i]\ Rotation\ [n_i, \alpha_i]\ is\ the\ x_i\ rotary\ motion.$

Therefore;

$$Trans_{z,\theta} \rightarrow (2)\ Trans_{z,d} \rightarrow (3)\ Trans_{n,a} \rightarrow (4)\ Trans_{n,\alpha} \quad (1)$$

The matrices associated with these operations are:

$$T_{zi-1}(d_i) = \begin{bmatrix} 1 & 0 & 0 & 0 \\ 0 & 1 & 0 & 0 \\ 0 & 0 & 1 & di \\ 0 & 0 & 0 & 1 \end{bmatrix} \quad (2)$$

$$R_{zi-1}(\theta_i) = \begin{bmatrix} cos\theta_i & -sin\theta_i & 0 & 0 \\ sin\theta_i & cos\theta_i & 0 & 0 \\ 0 & 0 & 1 & 0 \\ 0 & 0 & 0 & 1 \end{bmatrix} \quad (3)$$

$$T_{xi}(a_i) = \begin{bmatrix} 1 & 0 & 0 & a_i \\ 0 & 1 & 0 & 0 \\ 0 & 0 & 1 & 0 \\ 0 & 0 & 0 & 1 \end{bmatrix} \quad (4)$$

$$R_{xi}(\alpha_i) = \begin{bmatrix} 1 & 0 & 0 & 0 \\ 0 & cos\alpha_i & -sin\alpha_i & 0 \\ 0 & sin\alpha_i & cos\alpha_i & 0 \\ 0 & 0 & 0 & 1 \end{bmatrix} \quad (5)$$

Only the final modification pertaining to the twist angle transformation is being made to simplify the overall depiction of the segment. The arm matrix A is the result of multiplying these four transformations.

$$Arm_i = Trans_{z,d}Trans_{z,\theta}Trans_{n,a}Trans_{n,\alpha} \quad (6)$$

$$Arm_i = \begin{bmatrix} 1 & 0 & 0 & 0 \\ 0 & 1 & 0 & 0 \\ 0 & 0 & 1 & di \\ 0 & 0 & 0 & 1 \end{bmatrix} \begin{bmatrix} cos\theta i & -sin\theta i & 0 & 0 \\ sin\theta i & cos\theta i & 0 & 0 \\ 0 & 0 & 1 & 0 \\ 0 & 0 & 0 & 1 \end{bmatrix} \begin{bmatrix} 1 & 0 & 0 & ai \\ 0 & 1 & 0 & 0 \\ 0 & 0 & 1 & 0 \\ 0 & 0 & 0 & 1 \end{bmatrix} \begin{bmatrix} 0 & 0 & 0 & 0 \\ 0 & cos\alpha i & -sin\alpha i & 0 \\ 0 & sin\alpha i & cos\alpha i & 0 \\ 0 & 0 & 0 & 1 \end{bmatrix}$$

$$Arm_i = \begin{bmatrix} cos\theta i & -sin\theta i.cos\alpha i & sin\theta i.sin\alpha i & ai.cos\theta i \\ sin\theta i & cos\theta i.cos\alpha i & -cos\theta i.sin\alpha i & ai.sin\theta i \\ 0 & sin\alpha i & cos\alpha i & di \\ 0 & 0 & 0 & 1 \end{bmatrix} \quad (7)$$

The value of θ is correlated with the extension of the actuator, measured in millimeters, as expressed by Equation (8).

$$\theta = tan^{-1}\left[\frac{2\Delta_x}{D}\right] \quad (8)$$

The $\Delta_x$represents the incremental extension, either positive or negative, of a linear prismatic actuator. D refers to the diameter of the disc segment. The value of the twist angle α and the corresponding matrix Equation (9) will be determined by the combination of four-bit control.

$$Twist(bit,bit,bit,bit)_{ni,\alpha i} = \begin{bmatrix} 1 & 0 & 0 & 0 \\ 0 & cos\alpha_i & -sin\alpha_i & 0 \\ 0 & sin\alpha_i & cos\alpha_i & 0 \\ 0 & 0 & 0 & 1 \end{bmatrix} \quad (9)$$

The value of the twist angle α and the corresponding matrix equations (Equation (10) to Equation (16)) are determined by the state of the bit sequence.

$$Twist_{90°}(1,0,0,0) = \begin{bmatrix} 1 & 0 & 0 & 0 \\ 0 & 0 & -1 & 0 \\ 0 & 1 & 0 & 0 \\ 0 & 0 & 0 & 1 \end{bmatrix} \quad (10)$$

$$Twist_{135°}(1,1,0,0) = \begin{bmatrix} 1 & 0 & 0 & 0 \\ 0 & -0.707 & 0.707 & 0 \\ 0 & 0.707 & -0.707 & 0 \\ 0 & 0 & 0 & 1 \end{bmatrix} \quad (11)$$

$$Twist_{180°}(0,1,0,0) = \begin{bmatrix} 1 & 0 & 0 & 0 \\ 0 & 0 & 1 & 0 \\ 0 & -1 & 0 & 0 \\ 0 & 0 & 0 & 1 \end{bmatrix} \quad (12)$$

$$Twist_{225^\circ}(0,1,1,0) = \begin{bmatrix} 1 & 0 & 0 & 0 \\ 0 & -0.707 & 0.707 & 0 \\ 0 & -0.707 & 0.707 & 0 \\ 0 & 0 & 0 & 1 \end{bmatrix} \quad (13)$$

$$Twist_{270^\circ}(0,0,1,0) = \begin{bmatrix} 1 & 0 & 0 & 0 \\ 0 & 0 & 1 & 0 \\ 0 & -1 & 0 & 0 \\ 0 & 0 & 0 & 1 \end{bmatrix} \quad (14)$$

$$Twist_{315^\circ}(0,0,1,1) = \begin{bmatrix} 1 & 0 & 0 & 0 \\ 0 & 0.707 & 0.707 & 0 \\ 0 & -0.707 & 0.707 & 0 \\ 0 & 0 & 0 & 1 \end{bmatrix} \quad (15)$$

$$Twist_{360^\circ}(0,0,0,1) = \begin{bmatrix} 1 & 0 & 0 & 0 \\ 0 & 1 & 0 & 0 \\ 0 & 0 & 1 & 0 \\ 0 & 0 & 0 & 1 \end{bmatrix} \quad (16)$$

The simplified arm matrix A_i is Equation (17).

$$Arm_i = Rot_{z,\theta i}.Tran_{z,di}.Tran_{n,ai}.Twist(bit,bit,bit,bit)_{n,\alpha i} \quad (17)$$

The arm matrix typically represents a single degree of freedom. However, in this case, it represents the whole module or segment of the robot, denoted as $Arm_i = Module_i$

$$Module_i = Rot_{z,\theta i}.Tran_{z,di}.Tran_{n,ai}.Twist(bit,bit,bit,bit)_{n,\alpha i} \quad (18)$$

The positional relationship between body i and body $i-1$ can be expressed using a position matrix, denoted by the symbol M. The matrix is employed to transform a point from frame i to $i-1$, based on the NOAP representation.

$$Trans^n_i = \prod_{i=1}^{n} Module^i_{i-1} \; Module^{i+1}_{i} \ldots Module^n_{i+1} \quad (19)$$

$$Trans^n_i = \begin{bmatrix} n_x & o_x & a_x & P_x \\ n_y & o_y & a_y & P_y \\ n_z & o_z & a_z & P_z \\ 0 & 0 & 0 & 1 \end{bmatrix} \quad (20)$$

The yaw ϕ, pitch θ, and roll ψ for this twist module may be determined from matrix Equation (21) to Equation (23) to provide the position and orientation representation.

$$\phi = atan2(n_y, n_x) \quad (21)$$

$$\theta = atan2(-n_z, cos\phi.n_z + sin\phi.n_y) \quad (22)$$

$$\psi = atan2(sin\phi.a_x - cos\phi.a_y, -sin\phi.o_x + cos\phi.o_y) \quad (23)$$

The twist angle α is determined by the combination of four (4) actuation systems. The twist angle α is the angle formed between the Z reference axis and the Z transition axis around the X transition axis. By activating actuator number one, the frame rotates about 90°. When both actuators 1 and 2 are energized, the transition frame will spin an additional 135°, as seen in Figure 7. Please consult Table 1 and Table 2 for comprehensive information on the transition axis

rotation and the corresponding determined twist angle [18], [19].

Table 1 Assignment of D-H Frames with Varying Twist Angles

Bang-Bang Four Bit							
A1	1	1	0	0	0	0	0
A2	0	1	1	1	0	0	0
A3	0	0	0	1	1	1	0
A4	0	0	0	0	0	1	1
$\boldsymbol{\alpha_i}$	90°	135°	180°	225°	270°	315°	360°

Table 2 Twist Angle Variation for a Single Module

Variable Twist Angle, $\boldsymbol{\alpha}$							
$\boldsymbol{\alpha_i}$	90°	135°	180°	225°	270°	315°	360°
$\boldsymbol{cos(\alpha_i)}$	0	-0.707	-1	-0.707	0	0.707	1
$\boldsymbol{sin(\alpha_i)}$	1	0.707	0	-0.707	-1	-0.707	0
$\boldsymbol{d_i}$	0	0	0	0	0	0	0
$\boldsymbol{\theta_i}$	15°	15°	15°	15°	15°	15°	15°
$\boldsymbol{a_i}$	25	25	25	25	25	25	25

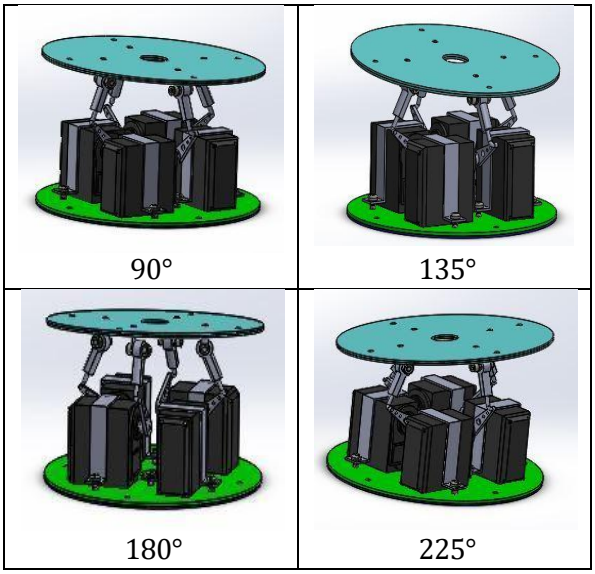

Figure 7. Sequence Operation based on Variable Twist Angle

4. PHYSICAL MODELING OF SINGLE MODULE

Prior understanding of system design principles, including complex mathematical equations and algorithms, is essential for the production and development of a four-bar linkage model based on parallel module. The physical modeling and simulation of single module may be accomplished by utilizing the virtual robot experimental platform, such as Maplesoft, which encompasses Maple and MapleSim software [20] or MATLAB. Additionally, it is necessary to create a geometric design of the four-bar connection of single module using Computer-Aided Design software.

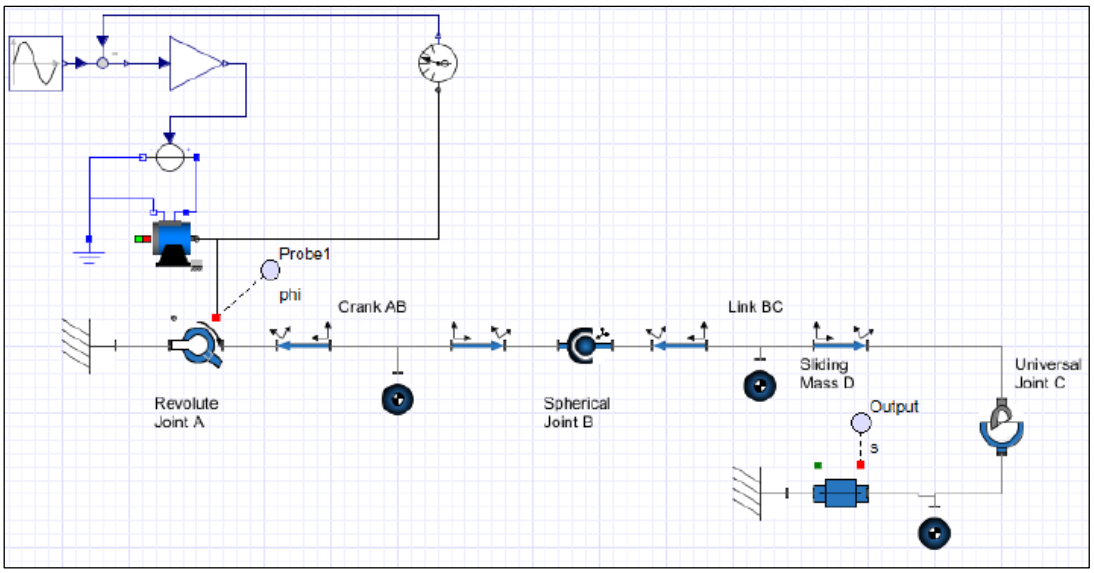

Figure 8. Model of 4-Bar Linkage in MapleSim

This will facilitate the ongoing use of virtual prototyping, specifically for simulation purposes within the MapleSim program. Therefore, the CAD design is connected to MapleSim to do model prototyping simulations. Upon completion of the control component, Maplesoft will generate C code automatically. Figure 8 depicts the first design depiction of a solitary module.

Figures 9 and Figure 10 illustrate the approach for accomplishing physical modelling and gait configuration.

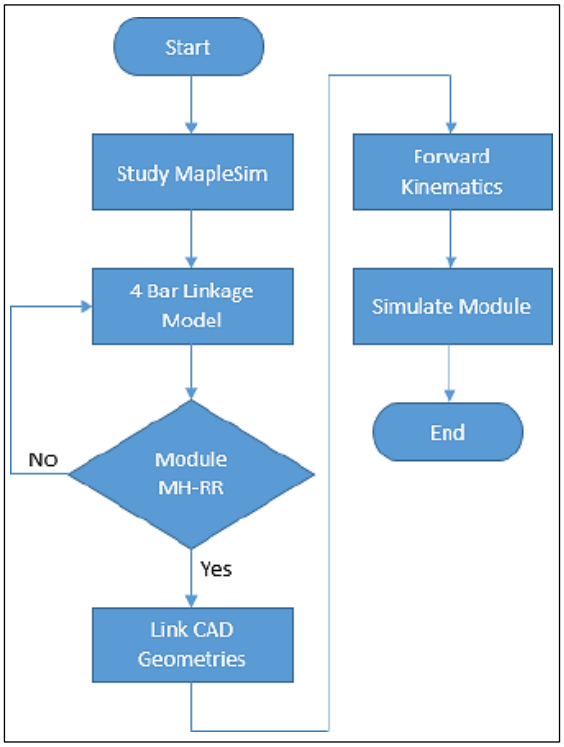

Figure 9. Single Module Physical Modeling using MapleSim

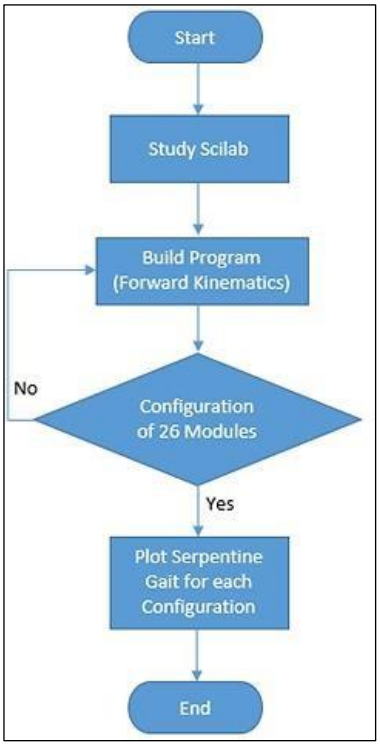

Figure 10. Gait Configuration using Scilab

The variable twist angle technique is widely recognized as the D-H approach Simplification module [9][10]. Several outcomes are presented below.

i. Twist Angle, α(i) = 0°
At a twist angle of 0º, the four actuators remain in their initial locations, indicating that none of the actuators have been activated, as seen in Figure 11.

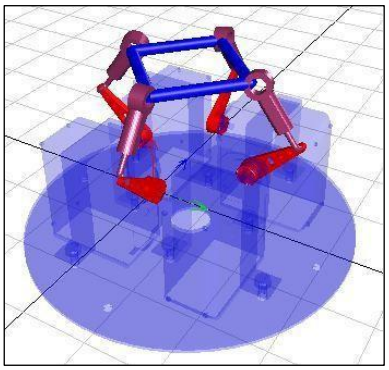

Figure 11. Twist Angle 0°

ii. Twist Angle, α (i)=135° & α(i)=315°
Servo motor 1 and servo motor 2 have activated Module 1 to Module 13 in the prescribed configuration (see to Table 3) to produce a twist angle, α, of 135º (as depicted in Figure 12). Afterwards, servo motor 3 and servo motor 4 are employed to activate Module 14 via Module 26, leading to the measurement of the twist angle, α, which is set at 315º, as seen in Figure 13.

Table 3 Gait Configuration

Module (i)	**Actuator**				**D-H Parameters**			
	1	2	3	4	α	d (mm)	θ	a (mm)
1-13	1	1	0	0	135°	0	15°	25
14-26	0	0	1	1	315°	0	15°	25

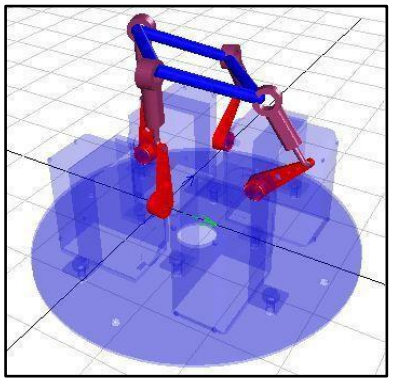

Figure 12. Twist Angle 135°

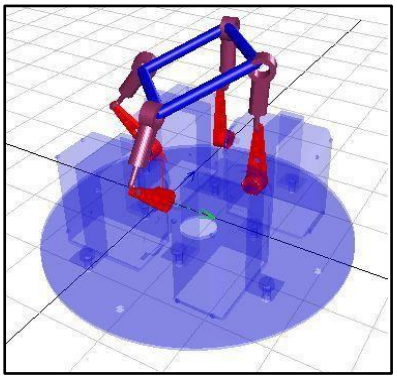

Figure 13. Twist Angle 315°

The twist angle may be measured in increments of 45 degrees, ranging from zero to 360 degrees. The indexing incremental movement is achieved by controlling the bit sequence of each pair of actuators, as seen in the findings. This module has the capability to conduct incremental orientation at 45-degree angles. When it is installed as part of a system, it allows for flexible three-dimensional flexure.

5. GAIT CONFIGURATION FOR FULL MODULE OF HYPER REDUNDANT ROBOT

The diagram below illustrates the many sinuous movements of the Modular Hyper-Redundant Robot in Scilab [21]. Each motion in the Figures is composed of 26 modules of a Hyper-Redundant Robot. To achieve a seamless serpentine motion in the shape of a "S," a total of 26 modules are required. A total of 39 distinct motions may be effortlessly mimicked utilizing a set of 26 components.

i. Configurations 1 to 14
This is the consecutive advancement of serpentine movement from Serpentine Configuration 1 to Serpentine Configuration 14. Figure 14 illustrates modifications occurring between Module 13 and Module 26.

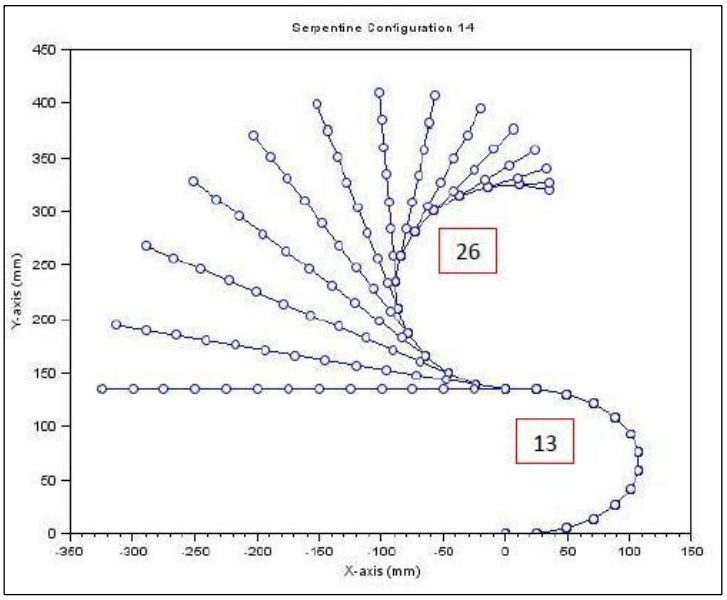

Figure 14. Sequential Transition from Serpentine Configuration 1 to Serpentine Configuration 14, Resulting in a Serpentine Motion

ii. Configuration 15-26
This represents the consecutive advancement from Serpentine Configuration 15 to Serpentine Configuration 26, including a serpentine motion. Figure 15 illustrates the modifications that occur between Module 1 and Module 12.

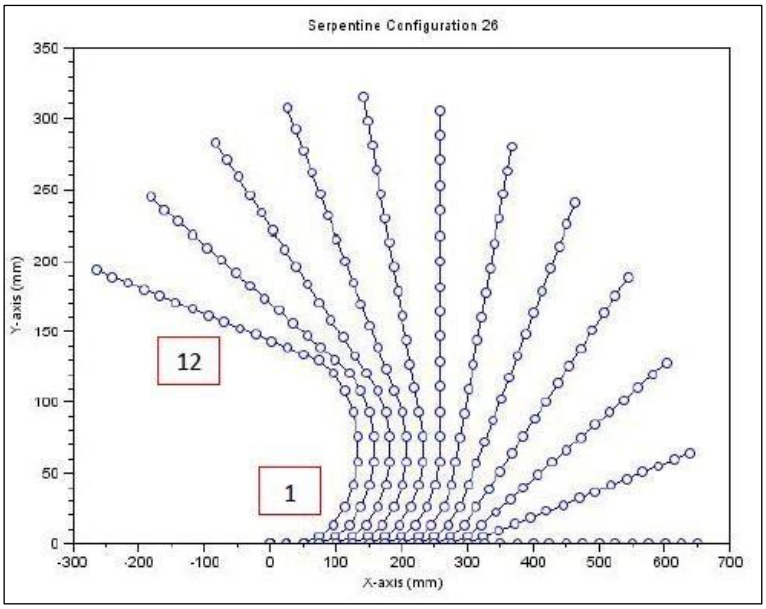

Figure 15. Transitioning from Serpentine Configuration 15 to Serpentine Configuration 26 by a Series of Serpentine Motions

Enabling configuration from 1-39 allows for the realisation of the whole sine wave's S form. This demonstrates that a basic kinematic model of the hyper redundant module, when joined in a certain number, may generate complicated shapes such as a S shape in three dimensions.

5.1 Discussion

The motion of a flying disc is controlled using the notion of bang-bang control, which is based on a single module. Changing the activation of the actuator may result in a change in the bending of the flying disc. A single module consists of four actuators. The flying disc may easily change its position based on the specific pair actuation sequences. The flying disc can move with flexibility within a range of 0° to 360°. The combination of a universal joint enables seamless motion by allowing the flying disc to flex individually. The ball joint creates a gap between its components, allowing it to withstand tremendous pressure and sustain weight while maintaining the ability to move freely in any direction.

The use of four bar links aimed to enhance the manoeuvrability and alignment capabilities of the flying disc. The four-bar links can translate and maintain a fixed position, provide support, or serve as a structure for Modular Hyper Redundant Robot (MHRR). When the actuator undergoes a 180° rotation, it can exert force to either push or pull the ball joint and flying disc. The servo motors of the MH-RR have the capability to rotate within a range of 0° to 180°. The actuator moves in a horizontal direction, either from left to right or from the front view of the servo motor. The trajectory of a flying disc's three-dimensional movement is determined by the motion of the actuator system.

On the other hand, a single module will perform repetitive actions to create a collection of modular systems. The MHRR project consists of 7 components that are integrated to form a single system resembling a snake-like robot. The integration of modules yields a diverse range of

applications that may be implemented on it. For instance, devices such as manipulators and robot arms.

5.2 Summary

Using four actuators in a single robot module can be an important design choice for several reasons, depending on the desired functionality of the robot. Here are some potential benefits:

i. Increased Degrees of Freedom (DOF): With three linear actuators, a module can typically only achieve movement along three linear axes (X, Y, Z). Adding a fourth actuator allows for additional control, potentially enabling:
   - Rotational movement around an axis
   - Telescoping or extending an arm segment.
   - Differential movement for more complex maneuver.

ii. Enhanced Modularity and Configurability: A four-actuator design could allow a single module to perform a wider range of tasks. This can be beneficial for modular robots where modules can be connected in different configurations to achieve different functionalities.

iii. Improved Stability and Load Capacity: By strategically placing four actuators, you can create a more stable structure for the module, especially when carrying heavier payloads. The additional actuator can provide more balanced forces and support for the module's movement.

iv. Specific Movement Patterns: Depending on the actuator arrangement, four actuators can enable the module to follow specific movement patterns. For example, a square or diamond-shaped CONFIGURATION with four actuators could allow for precise crawling or inchworm-like motion. However, it's important to consider the downsides as well:

v. Increased Complexity: Adding an actuator increases the complexity of the design, potentially requiring more control systems, wiring, and power consumption.

vi. Potential for Redundancy: Depending on the desired movement, four actuators might introduce redundancy. Careful design and control algorithms are needed to avoid conflicting movements from the actuators.

Overall, the decision of using four actuators depends on the specific needs of your robot design. If the benefits of increased DOF, stability, or specific movement patterns outweigh the added complexity and cost, then a four-actuator design can be a valuable choice.

6. CONCLUSION & FUTURE WORK

The Variable Twist Angle for a Single Module in a Hyper-Redundant Robot achieved by four-bar linkage mechanism or linear actuation. This module utilises a parallel design idea, employing a symmetric configuration of four actuators that serve as both muscle and framework, providing both flexibility and stability. The modularity of this architecture allows for increased flexibility, particularly when integrating separate modules into a larger system.

The variable twist angle modeling of a four-degree-of-freedom (4-DOF) robotic system into a single module arm matrix enables precise manipulation, allowing for control over position and orientation, including pitch and yaw. This module serves as a precursor to the upcoming iteration of a versatile end effector capable of several modes of operation.

This studied focus on analysing the Variable Twist Angle Single Module, which is located at the end-effector of a serial industrial robot and was inspired by the Stewart Platform. Each component of the module is composed of four linear actuators that are capable of bending and moving easily.

Due to its adaptability, a Variable Twist Angle Module was selected for its ability to function in crowded and restricted environments. The advantage of using these style-robots and accessible places may need complex movements of inflexible platforms, which might potentially surpass the limitations of the joints. Utilising flexible manipulators not only reduces examination time but also minimises energy usage.

The design, modeling, control, and teleoperation of serial and hyper-redundant robots can lead to future applications and benefits. These robots can be useful for inspection of industrial facilities, operative tasks, and hazardous environments like boiler rooms or nuclear core reactors. They can also serve as accessory manipulators for activities requiring fault tolerance, such as space exploration, as they can reconfigure if actuators fail. Additionally, highly articulated robots are interesting for research and educational purposes as they utilize traditional kinematics of traditional and industrial manipulators to their maximum expression.

REFERENCES

[1] L. A. Ballard, S. ŝabanović, J. Kaur, and S. Milojević, "George Charles Devol, Jr," *IEEE Robot. Autom. Mag.*, vol. 19, no. 3, 2012, doi: 10.1109/MRA.2012.2206672.

[2] G. S. Chirikjian and J. W. Burdick, "Hyper-Redundant Robot Mechanisms and Their Applications," *IEEE/RSJ Int. Work. Intell. Robot. Syst.*, no. 91, pp. 185–190, 1991, doi: 10.1109/IROS.1991.174447.

[3] G. S. Chirikjian and J. W. Burdick, "Design and Experiments with a 30 DOF Robot," *IEEE Int. Conf. Robot. Autom.*, no. 1, pp. 113–119, 1993, doi: 10.1109/ROBOT.1993.291862.

[4] Y. Zhao, X. Song, X. Zhang, and X. Lu, "A Hyper-redundant Elephant's Trunk Robot with an Open Structure: Design, Kinematics, Control and Prototype," *Chinese J. Mech. Eng. (English Ed.*, vol. 33, no. 1, pp. 1–19, 2020, doi: 10.1186/s10033-020-00509-4.

[5] Zhao-cai Du, G.-Y. Ouyang, J. Xue, and Y. Yao, "A Review on Kinematic, Workspace, Trajectory Planning and Path Planning of Hyper-Redundant Manipulators," in *10th IEEE International Conference on CYBER Technology in Automation, Control, and Intelligent Systems*, 2020, pp. 444–449.

[6] D. Sosa-Méndez, E. Lugo-González, M. Arias-Montiel, and R. A. García-García, "ADAMS-MATLAB Co-Simulation for Kinematics, Dynamics, and Control of the Stewart-Gough Platform," *Int. J. Adv. Robot. Syst.*, vol. 14, no. 4, 2017, doi: 10.1177/1729881417719824.

[7] L. Yan, W. Xu, Z. Hu, and B. Liang, "Virtual-Base Modeling and Coordinated Control of a Dual-Arm Space Robot for Target Capturing and Manipulation," *Multibody Syst. Dyn.*, vol. 45, no. 4, pp. 431–455, 2019, doi: 10.1007/s11044-018-09647-z.

[8] A. Martín-Barrio, J. J. Roldán-Gómez, I. Rodríguez, J. Del Cerro, and A. Barrientos, "Design of a hyper-redundant robot and teleoperation using mixed reality for inspection tasks," *Sensors (Switzerland)*, vol. 20, no. 8, 2020, doi: 10.3390/s20082181.

[9] L. Huang, B. Liu, L. Yin, P. Zeng, and Y. Yang, "Design and validation of a novel cable-driven hyper-redundant robot based on decoupled joints," *J. Robot.*, vol. 2021, 2021, doi: 10.1155/2021/5124816.

[10] A. Martín-Barrio, J. J. Roldán, S. Terrile, J. del Cerro, and A. Barrientos, "Application of immersive technologies and natural language to hyper-redundant robot teleoperation," *Virtual Real.*, vol. 24, no. 3, pp. 541–555, 2020, doi: 10.1007/s10055-019-00414-9.

[11] L. Tang, J. Wang, Y. Zheng, G. Gu, L. Zhu, and X. Zhu, "Design of a cable-driven hyper-redundant robot with experimental validation," *Int. J. Adv. Robot. Syst.*, vol. 14, no. 5, pp. 1–12, 2017, doi: 10.1177/1729881417734458.

[12] J. Peng, W. Xu, T. Yang, Z. Hu, and B. Liang, "Dynamic modeling and trajectory tracking control method of segmented linkage cable-driven hyper-redundant robot," *Nonlinear Dyn.*, vol. 101, no. 1, 2020, doi: 10.1007/s11071-020-05764-7.

[13] C. Lapusan, C. Rad, and O. Hancu, "Kinematic analysis of a hyper-redundant robot with application in vertical farming," *IOP Conf. Ser. Mater. Sci. Eng.*, vol. 1190, no. 1, p. 012014, 2021, doi: 10.1088/1757-899x/1190/1/012014.

[14] S. C. Lauguico, R. S. Concepcion, D. D. MacAsaet, J. D. Alejandrino, A. A. Bandala, and E. P. Dadios, "Implementation of Inverse Kinematics for Crop-Harvesting Robotic Arm in Vertical Farming," 2019, doi: 10.1109/CIS-RAM47153.2019.9095774.

[15] T. Ding, B. Li, H. Liu, Y. Peng, and Y. Yang, "Planar Multi-Closed-Loop Hyper-Redundant Manipulator Using Extendable Tape Springs :," vol. 7, no. 3, pp. 6630–6637, 2022.

[16] A. S. Lafmejani *et al.*, "Kinematic modeling and trajectory tracking control of an octopus-inspired hyper-redundant robot," *IEEE Robot. Autom. Lett.*, vol. 5, no. 2, 2020, doi: 10.1109/LRA.2020.2976328.

[17] S. Said, A. S. Ismail, and I. Baharin, "Degree of Freedom Compression in Denavit - Hartenberg Modeling for Huge number of Degree of Freedom Biomimetic Robotic System," in *Science & Engineering Technology National Conference (SETNC)*, 2013, pp. 1–6.

[18] A. S. Ismail, S. Said, I. Baharin, and L. L. See, "Physical Modeling Active Four Bar Linkage for Modular Hyper-Redundant Robot," in *Science & Engineering Technology National Conference (SETNC)*, 2015, pp. 1–6.

[19] A. S. Ismail, S. Said, and I. Baharin, "Variable Twist Angle of Flexible Electromagnetic Hyper Redundant Robot," *Int. J. Sci. Eng. Res.*, vol. 4, no. 5, pp. 30–35, 2013.

[20] O. C. C., I. A. B., O. B. A., T. N. T., and O. O. R., "Model Design of 3-Link Robotic Manipulator Using Maplesim," *Int. J. Sci. Res. Sci. Technol.*, 2020, doi: 10.32628/ijsrst207449.

[21] B. Borowik, M. Pyrc, and M. Gruca, "Design and kinematical analysis of a robot supporting rehabilitation," *Prz. Elektrotechniczny*, vol. 99, no. 1, 2023, doi: 10.15199/48.2023.01.59.